

THE USE OF LASER RAMAN MICROPROBE SPECTROSCOPY FOR INVESTIGATING RESIDUAL SURFACE STRAIN IN SELECTED CERAMICS

Norman L. Hecht, University of Dayton Research Institute, 300 College Park,
Dayton, OH 45469-0172

Perry P. Yaney, Department of Physics, University of Dayton, 300 College Park,
Dayton, OH 45469-2314

George A. Graves, University of Dayton Research Institute, 300 College Park,
Dayton, OH 45469-0172

ABSTRACT

Machining, various processing procedures, and property measurements can generate residual strains in ceramic components. Depending on the composition, crystal structure, and application, the residual strain generated can enhance or degrade the ceramic. Laser Raman microprobe spectroscopy has been found to be an effective tool for investigating residual strain in ceramic components. Strain induced by stresses in a ceramic material can alter the Raman spectra by (a) the generation of additional spectral features, (b) relative changes in intensity or widths of the Raman lines, and (c) shifting or splitting of lines. Specifically, Raman spectroscopy is being used to investigate the residual surface strain generated during selected machining processes and flexural testing. These studies are centered on silicon carbide (SiC) and silicon nitride (Si₃N₄) ceramics and the residual surface strains introduced by different machining methods. The results show a strong correlation between the Raman linewidths and the residual surface stress.

To the extent authorized under the laws of the United States of America, all copyright interests in this publication are the property of The American Ceramic Society. Any duplication, reproduction, or republication of this publication or any part thereof, without the express written consent of The American Ceramic Society or fee paid to the Copyright Clearance Center, is prohibited.

INTRODUCTION

The University of Dayton (UD) has participated in an Oak Ridge National Laboratory (ORNL) sponsored project investigating the thermal-mechanical behavior of candidate ceramics for heat engine applications since December 1984. As part of this project, Raman microprobe spectroscopy is being used to monitor residual strains in candidate ceramics subject to different machining treatments, mechanical loading, and microindents. In the initial work, the Raman microprobe was used to study transformation toughened ZrO_2 -based ceramics. The Raman microprobe identified the extent and amount of phase transformation (tetragonal \rightarrow monoclinic) around cracks extending from Vickers indents [1]. In more recent work, the Raman microprobe was used to study the strain around Vickers indents and along the tensile surface of Si_3N_4 flexural test bars in a four-point bending fixture [2]. In the current work, the Raman microprobe is being used to study residual strain in SiC and Si_3N_4 flexural test bars machined by different methods. The correlations between machining methods, residual strain, and fracture strength were evaluated and the results obtained are presented.

BACKGROUND

The phenomenon of frequency-shifted scattered light was first predicted theoretically by A. Smekal in 1923 and was first observed experimentally in liquids by C. V. Raman in 1928 [3]. This effect is now known as Raman scattering. Raman spectroscopy provides information over the visible spectrum and requires no specimen preparation in contrast to the typical requirements of infrared absorption spectroscopy. However, before the discovery of the laser, the limitations of light sources available to induce scattering and factors resulting in degradation of signal levels, such as fluorescence, phosphorescence, and sample imperfections, restricted the use of Raman spectroscopy. Developments in dispersing and detection systems helped to improve signal levels and maintain interest in Raman spectroscopy as a laboratory curiosity. The advent of the laser in 1960 and its application to spectroscopy resulted in a resurgence of Raman spectroscopy. Laser sources provide a number of highly monochromatic excitation

lines capable of producing Raman spectra with good signal-to-noise ratio (SNR) from small sample areas. Laser Raman spectroscopy/microspectroscopy has since developed into an important analytical and complementary spectroscopic technique. A schematic of the UD laser Raman microprobe system is shown in Figure 1.

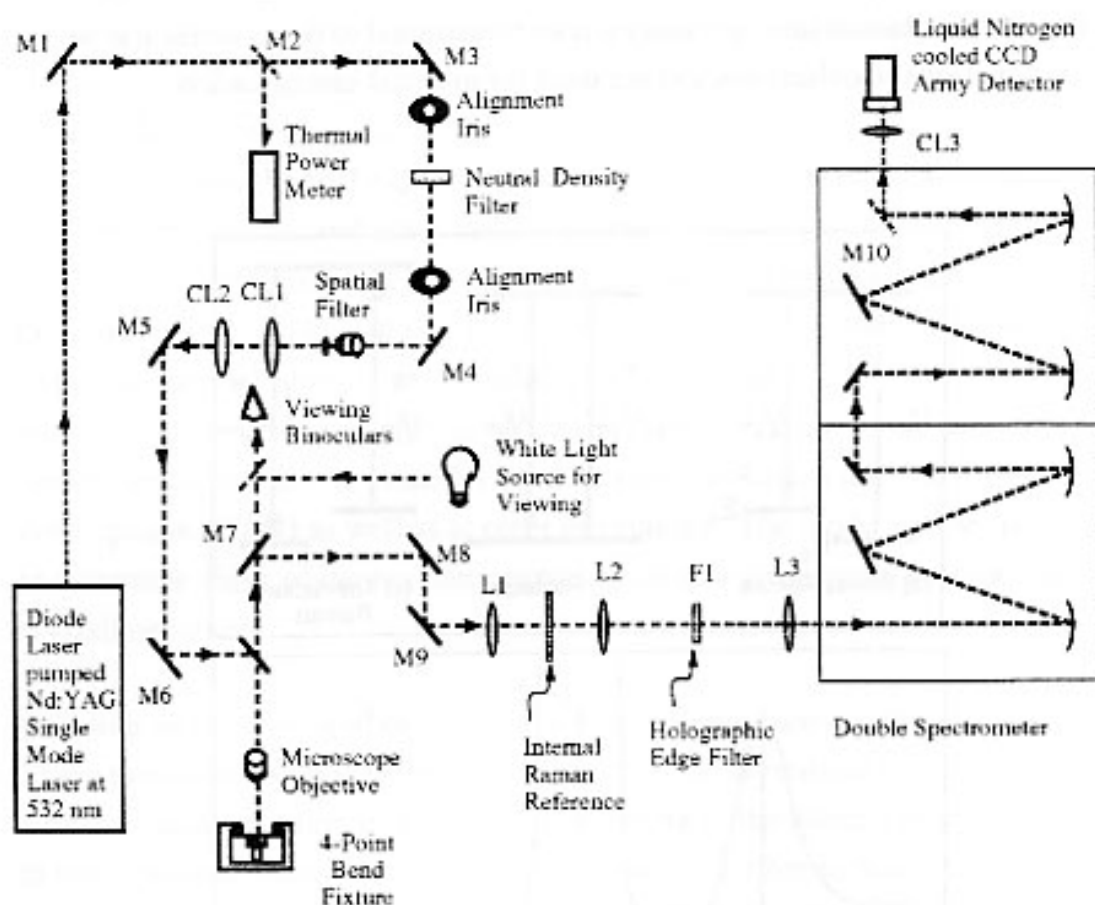


Figure 1. Laser Raman microprobe system in the Physics Department of the University of Dayton.

Monochromatic light interacts with the molecules or lattice structure of a probed material producing observable inelastically scattered light at shifted frequencies (Raman lines) and elastically scattered light at the same frequency as the incident beam (Rayleigh line). The frequencies of the Raman lines (about 10^{-12} times less intense from opaque solids than the incidence light) in the scattered light are

shifted from the incident frequency by precise values characteristic of the specific material (see Figure 2). These Raman spectra are due to the vibrations and/or rotation of the molecules or lattice vibrations in the solid. Both internal and external vibrations occur in crystalline solids. The internal vibrations involve molecular-like stretching and bending of the chemical bonds and the external vibrations involve partial rotations and translations of molecular units in the crystal lattice. Raman lines or "modes" can be assigned to these molecular or lattice vibrational mechanisms and are used for material identification.

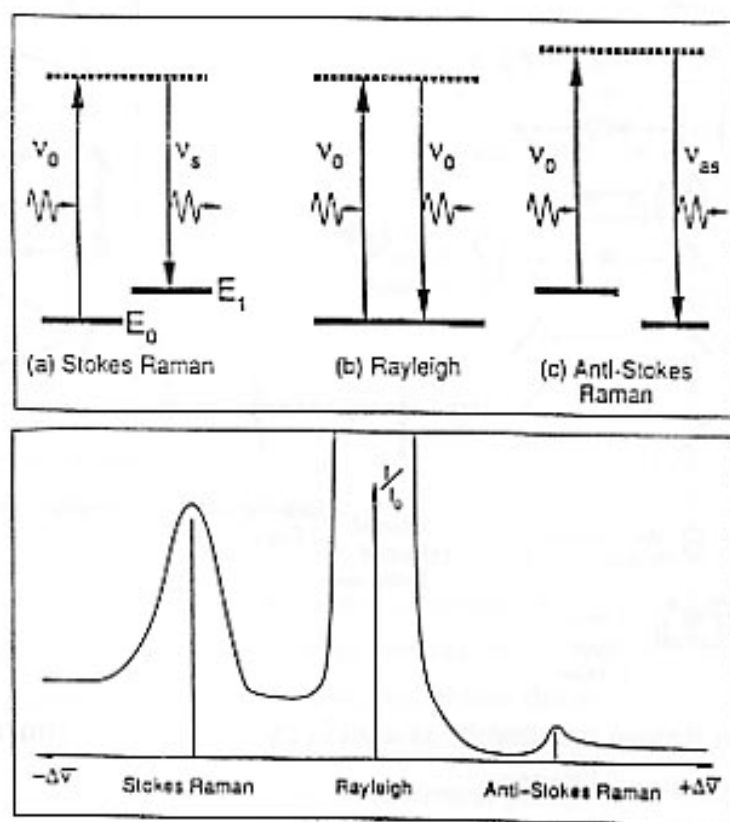


Figure 2. Light scattering process showing (a) Stokes Raman scattering, (b) Rayleigh scattering, and (c) anti-Stokes Raman scattering, and the corresponding spectrum. (The dotted energy "levels" are virtual states.)

Strain in a crystal can alter the Raman spectrum in the following ways [4]:

- (1) the generation of additional lines due to lowering of crystal symmetry,
- (2) intensity variations of the lines,
- (3) broadening of the line widths, and
- (4) shifting or splitting of the lines.

Strain in a crystal occurs in a number of situations for which changes in characteristic Raman spectra have been used as an investigative tool. In semiconductors, strain tends to occur by mismatches of the crystal parameters (lattice spacings, thermal expansion conditions) at epitaxial boundary layers [5]. For sapphire, silicon, and other materials strain is induced in the surface crystallites during polishing [6]. These strains are built into the lattice (referred to as intrinsic or residual strain) and produce Raman line shifts or broadenings. Externally applied stress induces strain, and flaws in a material (foreign inclusions, pores, and cracks) can be sites for stress concentrations and can cause Raman line shifts. A model to relate strain to Raman line shifts has been developed at UD [7] as well as at other institutions. The model can be used to determine shifts of internal lattice modes due to a given strain in a specific crystalline lattice.

Grinding and polishing of ceramic materials can introduce residual surface strain. These processes usually distort, to some extent, the crystalline lattice in the surface grains, resulting in a more rapid damping of the lattice vibrations, which in turn results in a broadening of the Raman lines. Different machining processes can introduce different levels of residual strain in the specimen surfaces resulting in different Raman linewidths. Inclusions of foreign atoms in the crystal lattice and other defects in the crystal structure can also introduce residual strains which may be reflected in the Raman spectra. As an example, Figure 3 shows a typical Raman line shift due to flexural strain in a Si_3N_4 test bar. Surfaces which have been only cut with a diamond saw and not ground typically give the narrowest lines. This is shown in Figure 4(a) for cubic CVD SiC. The change in this line after grinding treatments is shown in Figure 4(b). A more dramatic change due to built-in strain in the bulk material is the line splitting shown in Figure 4(c).

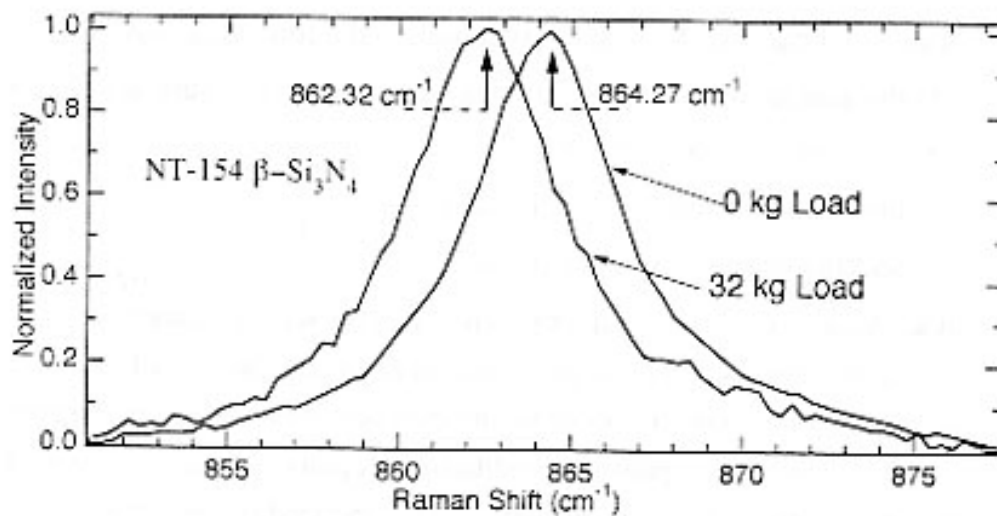


Figure 3. Shift of the 864 cm^{-1} line on the tension surface of a Si_3N_4 ceramic test specimen in a four-point bend jig due to a 32-kg load.

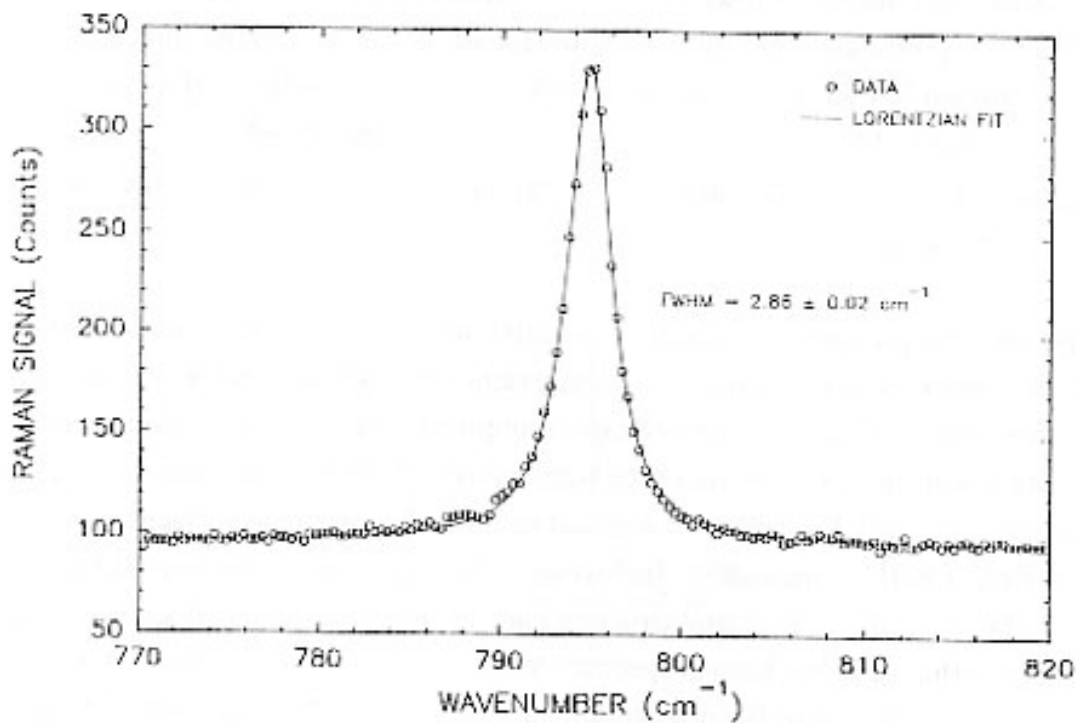


Figure 4. Raman TO line of cubic CVD SiC: (a) from a diamond cut, unpolished end of a Group 26 specimen.

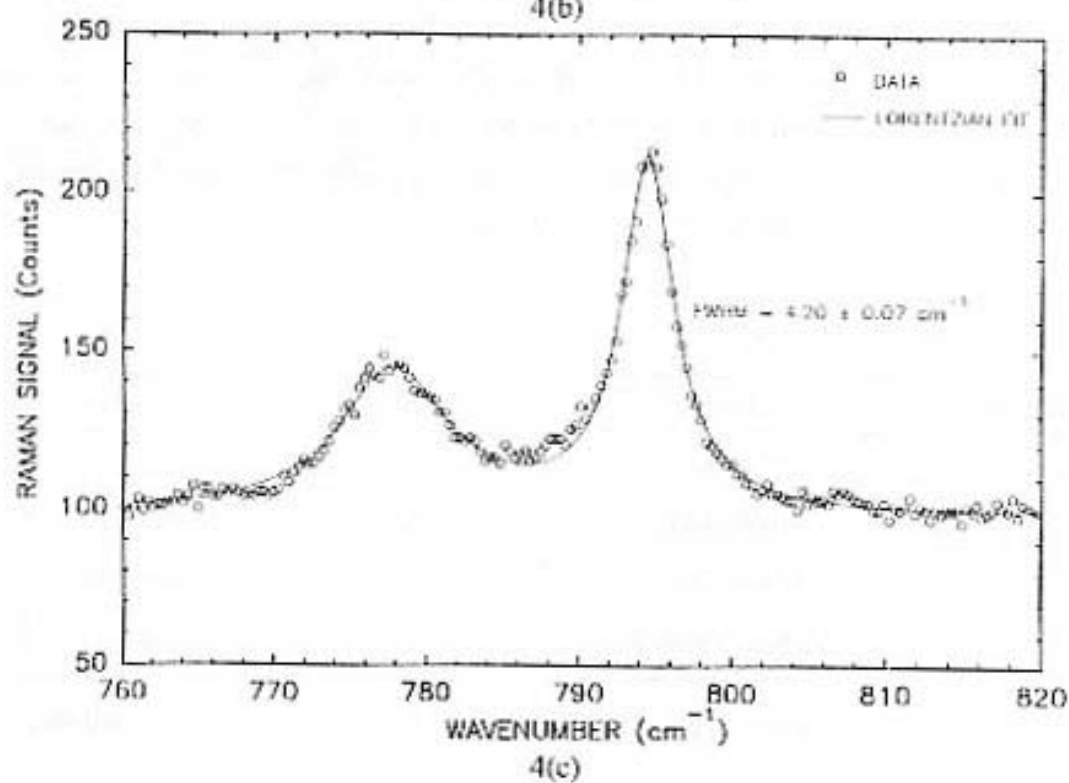
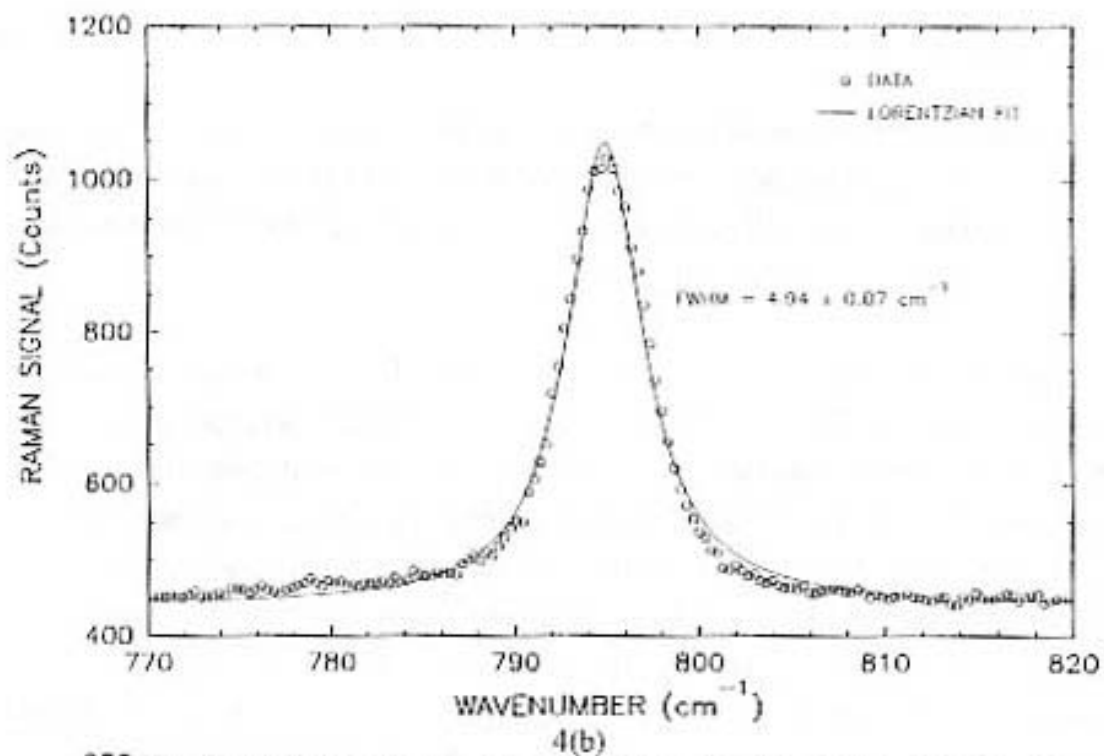


Figure 4. Raman TO line of cubic CVD SiC: (b) from the machined surface of a Group 23 specimen (see Table II) and (c) from one edge of a Group 27 specimen showing the presence of bulk strain.

EXPERIMENTAL PLAN

In our study to investigate selected machining effects, three different sets of four-point bend flexural test specimens (3 x 4 x 50 mm - ASTM C1161B) were used for evaluation: (a) four Allied Signal GS-44 Si_3N_4 , (b) 12 Morton International CVD SiC, and (c) 11 ORNL provided Si_3N_4 .

The different machining methods employed for the three test sets are outlined in Tables I through III. The residual strain in these flexural test specimens machined by different methods was investigated by Raman microprobe spectroscopy. The data obtained were acquired using a diode-laser pumped, doubled Nd:YAG laser. This laser provides 60 mW of highly stable, single-mode CW power at 532 nm. It has a bandwidth of less than 2 MHz. This allows us to acquire high quality data in a relatively short period of time. The spectrometer resolution and CCD array detector pixel size are the factors limiting the spectral resolution of the detection system. This amounts to an effective system bandwidth of about 0.6 cm^{-1} . High SNR and computer fitting techniques allow us to detect small changes in the widths of Raman lines, often less than 0.1 cm^{-1} . The data obtained for each specimen typically represents the average of 20 recorded positions spaced 5 to 15 μm apart.

Table I. Machining Treatments for GS-44

Number	Machining	Organization	Machine
1*	Baseline	Chand Kare Inc.	-
2**	Longitudinal	ORNL	Harrig NC
3	Transverse	ORNL	Harrig NC
4	Longitudinal Creep Feed	ORNL	Nicco

*The baseline specimen was final ground following ASTM C1161 but with a wheel that used a grit size finer 320.

**Final grind followed ASTM C1161.

Table II. Machining Treatments for CVD SiC Specimens*

Group	Wheel Type	Wheel Grit Size (μm)	Removal Rate mm/Pass	No. Passes	Total Amount Removed/Side (mm)
22	Norton SD150 R75B99E-1/4	100	0.005	5	0.025
23	Norton SD320 R75B99E-1/4	45	0.005	40	0.20
24	General Dia. CGD600 R75B-1/4	25	0.0025	10	0.025
25	Norton SD800 R50-1/32	18.5	0.0025	10	0.025
26	Norton ASD800 R75B56-1/4	18.5	0.0025	10	0.025
27	Norton D 3/6 mic R75B-1/4	3 to 6	0.0025	10	0.025

* All specimens longitudinally ground at Chand Kare Inc.

Table III. ORNL Si_3N_4 Specimens*

Billet Designation	Wheel Grit Size		Average Grinding Force (Newton)
	No.	(μm)	
13D21	320	44	38
07B21	80	177	90
06B21	320	44	75
06D21	150	105	93
13A21	500	33	135
07D21	150	105	101
12C22	320	44	28
09B21	600	30	122
03D21	320	44	33
03A21	320	44	65
14C21	500	33	237

* Specimens longitudinally ground at ORNL.

The spectral data were analyzed using a least squares fit of the Lorentzian line shape function to the data. For each data set, the peak height above background, the center frequency position, the full width at half maximum (FWHM), and the background level were fit as free parameters. The background level is designed to work with tilted backgrounds (i.e., it has a slope and y-intercept as free parameters). The fitting uncertainties in the widths were typically 1 to 5 percent. The poor optical quality of some specimens and relatively weak signal strengths account for the higher uncertainties.

Flexure strength was measured for all of the specimens used in these studies. The specimens were measured at 20°C in an Instron Universal Testing Machine 55RL23 following ASTM C1161. The strength values reported represent the average obtained for seven to ten specimens machined by the different methods cited.

Selection of Raman Lines for Analysis

For the GS-44 specimens, the width and the position of the 864 cm^{-1} line was investigated. Due to difficulties with fitting the width and the position of the 864 cm^{-1} line, the study was divided into two parts. In part one, the linewidths of 864 cm^{-1} line were measured. In part two, the positions of the lines with respect to a reference line of nitromethane were determined. In previous studies on Si_3N_4 [2,7], it was found that the 864 cm^{-1} line shifted up with applied compressive stress. The position measurements on the GS-44 specimens showed that the positions were directly correlated with the linewidth broadening. This confirmed the expectation that the broadening was due to residual compressive strains introduced by specimen machining.

The spectra from GS-44 Si_3N_4 specimens showed at least five additional lines that were absent from the spectrum of a typical $\beta\text{-Si}_3\text{N}_4$ specimen, such as Norton/TRW NT-154 Si_3N_4 (see Figure 5). These extra lines are present in the spectrum of $\alpha\text{-Si}_3\text{N}_4$ and correlate with the data of Wada et al. [8]. The spectra suggests that these specimens are a mixture of α - and β -phases.

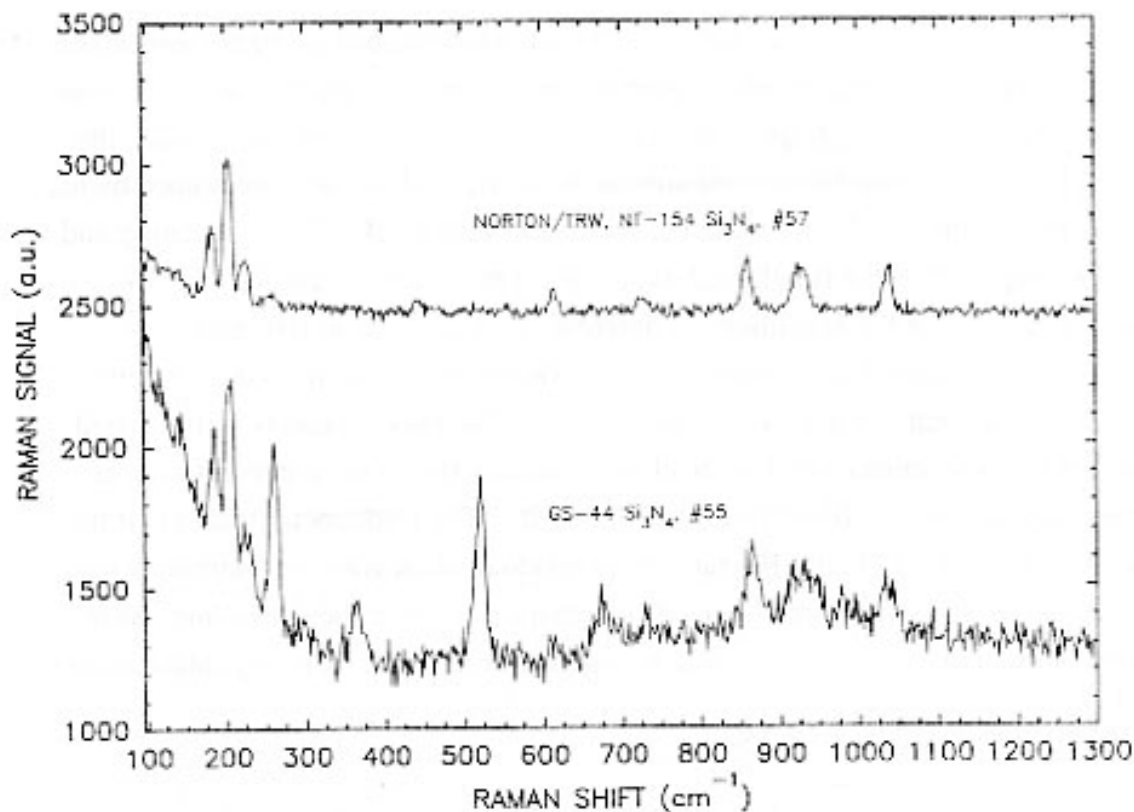


Figure 5. Survey Raman spectra of Norton/TRW NT-154 Si_3N_4 (upper trace) and GS-44 Si_3N_4 (lower trace).

For the CVD SiC specimens, the transverse optical (TO) mode at 795 cm^{-1} was studied. Two specimens from each of the groups were evaluated. Each specimen was probed on the two surfaces near one edge of the long dimension. All of the specimens probed showed a splitting of the TO line along the edge. The largest splittings were observed in specimens from Group 27 (see Figure 4c). Since both splitting and line broadening depend on the character and intensity of a bulk strain, correlations between the various parameters of the two split lines were studied. These correlations supported the contention that the splitting was due to residual bulk strain introduced prior to machining.

For the ORNL Si_3N_4 specimens, the Raman line at 449 cm^{-1} was used for evaluating line broadening. For these specimens, the Raman line for free silicon at 523 cm^{-1} was found and also used in this study. To better compare the results

in this phase of the study, a baseline spectrum was obtained using an unstrained silicon wafer. The silicon nitride Raman line at 449 cm^{-1} and the silicon Raman line at 523 cm^{-1} for each specimen were measured. In the past, the Raman line at 864 cm^{-1} was used for the measurements on Si_3N_4 . For the current specimens, the Raman line at 864 cm^{-1} was very broad and very weak. The broadening and weakening of this line is believed to be due, in part, to the presence of both α - and β - Si_3N_4 in the specimens. Therefore, a series of measurements were made to determine if there were any other Raman lines with the same or better sensitivity as that of the 864 cm^{-1} Raman line. The measurements were carried out on two specimens which were chosen because they were representative of the coarsest (80) and finest (600) grinding grits. The findings indicated that the sensitivity of the 449 cm^{-1} Raman line to residual strain was approximately the same as the 864 cm^{-1} Raman line. The signal levels from these two lines were quite similar, and the 449 cm^{-1} line was narrower and free from any interferences.

DISCUSSION OF RESULTS

The Raman line broadening measured for each category of flexural test specimens, the average flexural strength, and the corresponding machining variables used are compiled in Tables IV through VI.

Table IV. Summary Results for GS44*

Specimen No. and Machining Procedure	Raman Line Width (cm^{-1})	Average Flexural Strength (MPa)
#1 longitudinally ground at Chand Kare Inc.	13.68 ± 0.61	1160 ± 162
#2 longitudinally ground at ORNL	15.46 ± 0.81	1135 ± 55
#3 creep feed ground at ORNL	13.63 ± 1.29	1183 ± 71
#4 transversely ground at ORNL	15.61 ± 0.75	871 ± 71

* All specimens probed at $\sim 0.7\text{ mm}$ from edge.

Table V. Summary Results for CVD SiC

Specimen Group No.	Grit Size (μm)	Raman Linewidth (cm^{-1})	Average Flexural Strength (MPa)
22	100	3.20 ± 0.19	352 ± 29
23	45	3.45 ± 0.15	383 ± 23
24	25	3.11 ± 0.10	454 ± 17
25	18.5	3.05 ± 0.15	389 ± 32
26	18.5	2.87 ± 0.14	478 ± 52
27	3-6	2.83 ± 0.12	297 ± 65

Table VI. Summary Results for ORNL Si_3N_4

Billet Number	Wheel Grit No.	Average Grinding Force (Newton)	Average Flexural Strength MPa (m) [*]	Average Raman Linewidth	
				Si_3N_4 ^{**}	Si ^{***}
07B	80	90	571 (26)	4.35 ± 0.08	4.52 ± 0.04
07D	150	101	610 (24.4)	4.10 ± 0.04	3.82 ± 0.06
06D	150	93	700 (18.3)	4.24 ± 0.05	3.73 ± 0.08
03D	320	33	672 (30.2)	3.95 ± 0.03	3.66 ± 0.06
12C	320	28	758 (24.7)	4.10 ± 0.04	3.50 ± 0.08
06B	320	75	802 (47.9)	4.27 ± 0.04	3.76 ± 0.08
03A	320	65	816 (12.2)	3.14 ± 0.04	3.28 ± 0.07
13D	320	38	893 (26.4)	4.42 ± 0.05	3.68 ± 0.08
13A	500	135	892 (16.7)	4.15 ± 0.07	3.60 ± 0.07
14C	500	237	989 (30.9)	4.15 ± 0.04	3.79 ± 0.10
09B	600	122	1016 (20)	4.00 ± 0.09	3.77 ± 0.09

^{*} (m) = Weibull modulus

^{**} 449 cm^{-1} line

^{***} 523 cm^{-1} line

The GS-44 specimens were probed at two locations, one close to the chamfered edge and one at some distance from the edge (typically about 0.7 mm). These measurements were taken to determine if there was any difference between the tensile surface and the chamfer. The linewidths tended to be smaller at the chamfered site due to less machining.

The Raman linewidths given in Table IV for the GS-44 specimens were unusually large. This effect is believed to be due, in part, to the presence of the α - Si_3N_4 phase. Additionally, the 848 cm^{-1} line of α - Si_3N_4 interferes with the 864 cm^{-1} line of the β -phase to give a doublet. Moreover, energy dispersive spectroscopy (EDS) of these specimens showed the presence of free silicon, magnesium, iron, aluminum, and chlorine. The presence of a sufficient concentration of these impurities can cause stress in the test specimens, which can contribute to the observed linewidths. Nevertheless, the data in Table IV show that, as expected, the linewidth is independent of the machining direction and that the finer machining procedures produce the narrower lines and the highest strengths. Since narrower lines imply lower residual strain, this correlation indicates that machining can degrade the ceramic specimens and reduce their strength. Thus, it is observed that the flexural strength tends to be inversely related to the residual surface strain caused by machining effects.

CVD SiC

The high symmetry of the cubic lattice of CVD SiC gives a Raman spectrum with a two-fold degenerate TO line at 795 cm^{-1} and singly-degenerate longitudinal optical (LO) line 975 cm^{-1} . If the lattice symmetry of the CVD SiC is strongly deformed during processing or by the presence of residual strain, lattice symmetry can be lowered. The lower symmetry can cause additional lines to appear with the possible removal of the degeneracies of existing lines. Splitting of the TO line was observed, as described in the Experimental Plan section. At the same time, the LO line showed no splitting, as expected. This splitting was found on both ground and cut surfaces indicating that this behavior was

independent of the machining indicating that it was due to a residual bulk stress and the corresponding strain introduced during the growth of the material.

A bar graph showing the mean and standard deviations (of the mean) of the linewidth data measured for the SiC specimens from the different test groups is presented in Figure 6. The bars are plotted in the order of grinding fineness. The two bars on the extreme right side are for etched specimens from Group 23 and Group 27, respectively. Except for Group 23, the linewidths in Figure 6 show decreasing strain for the finer grit grinding wheels. Group 23 has the widest linewidth [see Figure 4(b)] and the highest residual surface strain which is attributed to the 40 passes used in the finishing process (four to eight times those of the other groups). The high number of passes introduced significantly more strain in the surface of the test specimens resulting in a reduced flexural strength, as shown in Table V.

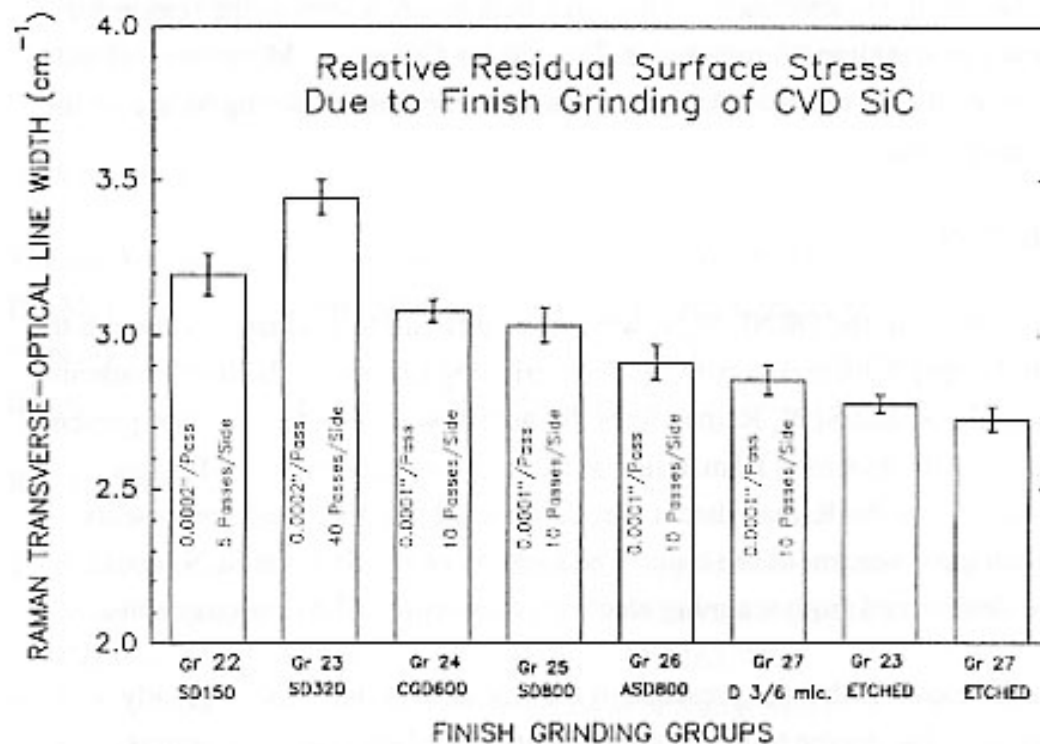


Figure 6. Average linewidths of the 795 cm⁻¹ line of CVD SiC showing relative residual surface stress due to the machining treatments given in Table III.

In order to better determine the source of line broadening, specimens from each group were etched to remove the surface layer. The widths for the etched specimens were lower than the widths measured for the machined specimens. These results strongly support the conclusion that the variation in linewidth is due to residual surface strain introduced by the grinding process. Currently, no theoretical model or data directly relating linewidth to actual residual strain values is available. Empirically, however, it is observed that line broadening due to residual strain is accompanied by line shifts. Since line shifts can be theoretically related to strain [7] and experimentally to stress [2], then it may be possible to calibrate line broadening in terms of residual stress for specific lines.

From measurements of the splitting of the 795 cm^{-1} line, it was found that the specimens from Group 27 showed the largest TO splitting. These findings suggest that the specimens from Group 27 contain considerably more bulk strain than the remaining specimens. This large bulk strain is seen as the reason for the low flexural strength reported in Table V for Group 27. Moreover this bulk strain may also be responsible for the scatter in the flexural strengths across the remaining groups.

ORNL Si_3N_4

The results from the ORNL Si_3N_4 were more difficult to evaluate. Although the flexural strength increased with the finer grinding treatment, the line broadening for both the Si and Si_3N_4 Raman lines did not show similar trends. The presence of free-Si with its strong Raman line at 523 cm^{-1} was not expected for this material. From the Raman data it was determined that the free-Si represents less than three percent of the bulk. The location of the Si in the Si_3N_4 could not be determined from scanning electron microscope (SEM) micrographs.

The implication is that the presence of the free and 'softer' silicon greatly complicates the degree to which strain is introduced into the Si_3N_4 grains. Within a given grit size, the Si linewidths follow (with one exception) the grinding force. Moreover, the largest two Si linewidths occur with the coarsest grits.

CONCLUSIONS

Laser Raman microprobe spectroscopy provides a means for detecting the presence of strains in solid specimens. This strain is revealed typically by broadening, shifting, or splitting of Raman lines. The presence of residual surface strain introduced by machining treatments is revealed in the broadening of the Raman lines. Studies show that this broadening is accompanied by slight line shifts. Systematic measurements of shifts of specific Raman lines due to applied stress show that these line positions increase with applied compressive stress. The line broadening due to machining is directly correlated with line positions which confirms that the residual surface strain is compressive.

The measurements required to reveal residual surface strains are accomplished by time-consuming, high-resolution Raman spectroscopy. There is considerable need for enhanced data acquisition techniques in order to begin the development of a larger database that includes a variety of materials. This database should include correlations with mechanical behavior and fractography.

ACKNOWLEDGMENTS

The authors would like to acknowledge the support of Dr. D. R. Johnson and Dr. M. E. Ferber of Martin Marietta at ORNL and the work of our graduate students N. D. Wolfe and M. Arif. We would also like to acknowledge the technical support of D. E. McCullum, D. W. Grant, and J. D. Wolf.

REFERENCES

1. M. Lander, S. Pruchnic, and P. P. Yaney, "Application of Laser Raman Macro-Microprobes Using Cylindrical Optics to the Study of Zirconia Ceramic Materials," *Bull. Am. Phys. Soc.* 32:2163, 1987.
2. P. P. Yaney and S. L. Ernst, "Investigation of Strain Mapping in Silicon Nitride Ceramic Using a Laser Raman Microprobe," *Bull. Am. Phys. Soc.* 37(9):1892, 1992.

3. R. S. Krishnan, "Historical Introduction," Chapter I in The Raman Effect, Vol. I: Principles, edited by A. Anderson (New York: Marcel Dekkar, Inc.), p. 2, 1971.
4. P. M. A. Sherwood, Vibrational Spectroscopy of Solids (London: Cambridge University Press), p. 3, 1972.
5. S. Nakashima and M. Hangyo, "Characterization of Semiconductor Materials by Raman Microprobe," *IEEE J. of Quantum Electronics* 25(5):965, 1989.
6. J. Rydzak and W. R. Cannon, "Fourier Transform Infrared Microscopy Method to Determine Stress in Sapphire," *J. Amer. Ceram. Soc.* 72(8):1559, 1989.
7. T. D. Fang and P. P. Yancy, "A Numerical Simulation of the Stress-Induced Shifts in the Raman Spectrum of β -Si₃N₄ Ceramic," *Bull. Am. Phys. Soc.* 38(7):1663, 1993.
8. N. Wada, S. Solin, J. Wong, and S. Prochazka, "Raman and IR Absorption Spectroscopic Studies on α , β , and Amorphous Si₃N₄," *J. Noncrystalline Solids* 43:7, 1983.